Available online at www.sciencedirect.com

Polymer 46 (2005) 2573–2578

polymer

www.elsevier.com/locate/polymer

Morphological and electronic consequences of modifications to the polymer anode 'PEDOT:PSS'

Henry J. Snaith, Henry Kenrick, Marco Chiesa, Richard H. Friend*

Cavendish Laboratory, Madingley Road, Cambridge CB3 0HE, UK

Received 23 July 2004; received in revised form 19 November 2004; accepted 25 January 2005

Abstract

We present a microscopic and electronic investigation of the polymeric anode poly(3,4-ethylenedioxythiophene):poly(styrenesulfonate) (PEDOT:PSS) used as an electrode in photovoltaic and single carrier diodes. PEDOT:PSS is processed from aqueous solution as a colloidal dispersion with excess PSS present. We modify the PEDOT:PSS solution by the addition of a high boiling point alcohol, glycerol, which is known to increase the conductivity of the spin-coated film. Atomic force microscopy indicates swelling and greater aggregation of the PEDOT-rich colloidal particles found in this system. Current–voltage characteristics of 'hole-transporting' diodes, formed with gold contacts, suggest less surface enrichment of PSS in the glycerol modified electrode. Through Kelvin probe microscopy, we find the surface potential of glycerol modified PEDOT:PSS decreases by approximately 0.12 eV, which we assign to a reduction in surface enrichment by PSS. Photovoltaic diodes, using a PFB:F8BT polymer blend as the photo-active layer, and glycerol modified PEDOT:PSS anodes are significantly improved as compared to those with unmodified PEDOT:PSS anodes. This is likely to be due to improved hole-injection from the active polymer film into the PEDOT:PSS anode. This emphasises the electronic consequences of the morphological reorientation of the PEDOT and PSS.

Keywords: PEDOT:PSS; Conducting polymers; Organic optoelectronics

1. Introduction

Solar power conversion efficiencies of over 3% are now routinely achieved for organic photovoltaic devices [1], and organic light emitting diodes have already reached commercial viability [2]. However, there still remain many mysteries concerning the operational characteristics of optoelectronic devices. Further to the choice of materials, the specific nano- and microstructure of polymer blends significantly influences the electronic properties of the system. Much work has been undertaken altering the morphology of the photoactive layer in order to optimise and study the device characteristics [3,4]. As well as understanding the processes occurring in the photoactive layer, it is important to understand the intricacies of the conductive electrodes. The metallic polymer blend, poly(3,4-ethylenedioxythiophene):poly(styrenesulfonate) (PEDOT:PSS), has been used successfully in photovoltaic devices and light emitting diodes as a hole-collecting or hole-injecting anode due to its high work function and electron blocking characteristics [5–7]. The use of PEDOT:PSS is also desirable as it increases the lifetime of optoelectronic devices [8], and in comparison with some inorganic oxide electrodes, the work function of the PEDOT:PSS is relatively stable, giving more reproducible device characteristics [9]. When modified to raise its conductivity PEDOT:PSS can be used efficiently as an anode in its own right [10]. However, due to its relatively low charge mobility, when compared to its inorganic counterparts, it is typically used in a bi-layer configuration with an indium tin oxide (ITO) contact. It has been reported that adding glycerol to PEDOT:PSS increases the conductivity and improves the efficiency of polymer light-emitting diodes [11]. Zhang et al. have shown that the efficiencies of photovoltaic devices are also improved [12]. However, for both these systems the devices were fabricated solely with PEDOT:PSS anodes and no ITO or metallic contact. In this

---

* Corresponding author. Tel.: +44 1223 337218; fax: +44 1223 353397.
E-mail address: rhf10@cam.ac.uk (R.H. Friend).

0032-3861/$ - see front matter © 2005 Published by Elsevier Ltd.
doi:10.1016/j.polymer.2005.01.077

case the improvement in efficiency can be simply related to the increase in conductivity.

PEDOT:PSS is an aqueous colloidal dispersion. The current model for the structure of a PEDOT:PSS film is that it consists of polymer dispersion particles which have a core shell morphology with a PSS-rich shell [13]. Furthermore, the PEDOT:PSS spin-coated film has been shown to vertically segregate, macroscopically, leading to a PSS-rich surface layer [14,15]. We note that the core-shell nature of the polymer nanoparticles is likely to limit the conductivity as there will be a charge blocking layer, of insulating PSS, at the grain boundaries. In this paper we investigate the morphological variation of the PEDOT:PSS anode when glycerol is added to the solution prior to film formation (this shall be referred to as G-PEDOT:PSS), and elucidate the electronic consequences of the morphological reorientation. We find the conductivity of PEDOT:PSS increases by three orders of magnitude upon the addition of glycerol. From atomic force microscopy it is apparent that the addition of glycerol results in swelling and aggregation of the polymer nanoparticles in the dried film. As reported below, this together with evidence for less surface enrichment by PSS, causes considerably altered behaviour in various diode structures.

2. Experimental

The semiconducting polymers used were poly(9,9-dioctylfluorene-co-benzothidiazole) (F8BT) as the electron transporting material, and poly(9,9′-dioctylfluorene-co-bis-*N*,*N*′-(4-butylphenyl)-bis-*N*,*N*′-phenyl-1,4-phenyldiamine) (PFB) as the hole transporting polymer. The chemical structure absorption and emission spectra are shown elsewhere [16]. PFB and F8BT were dissolved in chloroform separately at a concentration of 10 g/l and blend solutions of 1:1 PFB:F8BT by weight were mixed. An aqueous dispersion of the conductive polymer blend poly(3,4-ethylenedioxythiophene) poly(styrenesulfonate) (PEDOT:PSS) weight ratio of 1:16 PEDOT:PSS was used for the anode (Fig. 1).

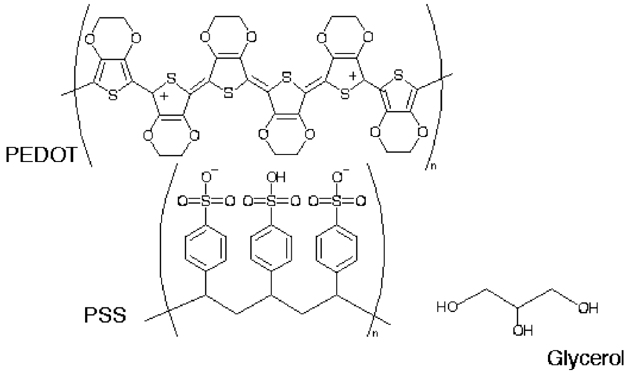

Fig. 1. Chemical structure of the materials used in the polymer anode: poly(3,4-ethylenedioxythiophene):poly(styrenesulfonate) (PEDOT:PSS) and glycerol which was optionally added.

Glycerol was optionally added to the PEDOT:PSS solution at a concentration of 8% glycerol by volume. This mixture will be referred to as G-PEDOT:PSS as well as dried films spin-coated from this solution. The PEDOT:PSS solution was spin-coated on pre-cleaned ITO substrates, unless otherwise stated, to give a thickness of approximately 50 nm. The polymer films were heated to 80 °C for 1 h, capped to reduce the rate of solvent evaporation in order to allow reorientation of the PEDOT:PSS, and for a further 30 min at 120 °C uncapped. The film thicknesses were measured using a stylus profilometer (Sloan Dektak IIA).

Atomic force microscopy (AFM), and photovoltaic device preparation and characterisation was performed as previously by the authors [16]. The Kelvin probe microscope set up used to measure the surface potential of films in ultra high vacuum was identical to that described by Burgi et al. [17]. PEDOT:PSS films were spin-coated onto ITO substrates, and the rig calibrated by measuring a gold film before and after sample measurements. Fourier transformed infra-red spectroscopy (FTIR) measurements were made in a nitrogen atmosphere using a bench top FTIR spectrometer (Nicolet 870, Thermo Electron). Samples were spin-coated onto brushed crystalline silicon wafers, which had been prepared in the same way as the ITO substrates.

The sheet resistivity was measured using a Karl Suss four-point probe rig in a nitrogen atmosphere. Micro-tunable electrode probes were applied at equal 2.5 mm distances along a straight line. A semiconductor parameter analyser (Agilent 4155C) was used to apply voltage at the two outside probes, where the applied current was measured, and measure the voltage across the sample between the two middle probes. Samples were prepared on pre-cleaned glass slides. The films used were thicker than in the devices (200 nm).

3. Results

Films were prepared from PEDOT:PSS solutions containing an excess of PSS (weight ratio of PEDOT to PSS 1:16). Films fabricated from this PEDOT:PSS are less conductive than from commercially available Baytron P (PEDOT:PSS weight ratio 5:8) but have been found to perform well as anodes in light emitting diode structures [18]. Our films showed an increase in conductivity by three orders of magnitude when modified with glycerol, the sheet resistance decreasing from 4.3×10^8 to 1.7×10^5 Ω/cm. It has been shown that adding glycerol to commercially available (Baytron P) PEDOT:PSS reduces its sheet resistance fivefold to approximately 1×10^3 Ω/cm [11].

From the atomic force microscopy images, Fig. 2, the PEDOT:PSS film is very smooth, having a vertical scale of 3 nm. However, there is a granular structure on the 40 nm length scale which can be assigned to the polymer

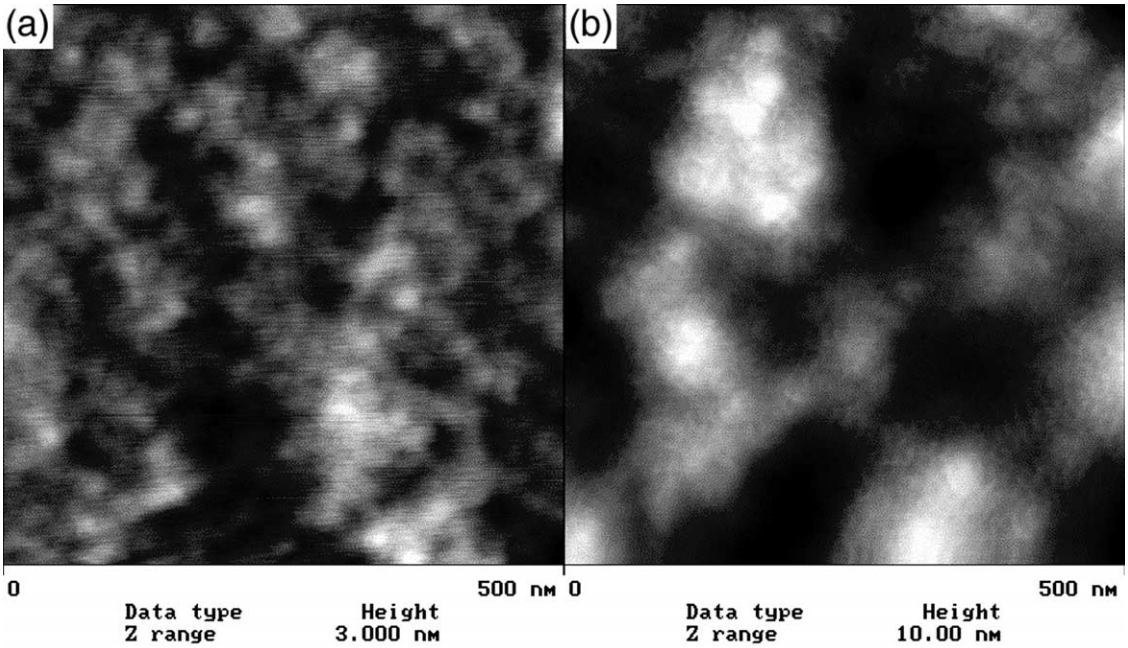

Fig. 2. AFM images of: (a) PEDOT:PSS and (b) G-PEDOT:PSS spin-coated on ITO-coated glass slides.

nanoparticles from the aqueous dispersion [19]. The surface of the G-PEDOT:PSS film appears more uneven at the micron length-scale, however the film is smoother on the nanometre scale. We can see that the small (40 nm) dispersion particles, which are clearly present in the PEDOT:PSS film, appear to have become 'swollen' and aggregated in the G-PEDOT:PSS film.

Fourier transform infra-red (FTIR) spectra for thin films of glycerol, G-PEDOT:PSS as spun, G-PEDOT:PSS annealed at 80 °C for 1 h and G-PEDOT:PSS annealed at 80 °C for 1 h followed by 120 °C for half an hour are shown in Fig. 3. The broad peak at 3360 cm^{-1} corresponds to the O–H stretching mode in the glycerol molecule, [20] this is not present in the annealed PEDOT:PSS or G-PEDOT:PSS films' spectra. It is clearly apparent that almost all the glycerol has left the film after annealing at 80 °C for 1 h and there is no significant residue after annealing at 120 °C.

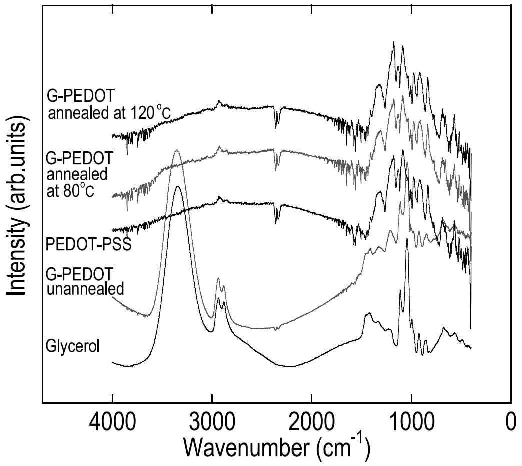

Fig. 3. Fourier transformed infrared (FTIR) absorption spectra for thin films of glycerol, G-PEDOT:PSS unannealed, PEDOT:PSS annealed 120 °C, G-PEDOT:PSS annealed 80 °C and G-PEDOT:PSS annealed 120 °C from bottom to top. The relative positions of each curve have been offset for ease of interpretation.

Kelvin probe microscope images show a significant difference when glycerol is added to PEDOT:PSS, Fig. 4. We first notice that with the addiction of glycerol the surface potential becomes marginally smoother over the whole film. However, this effect is not highly significant. Most notably, we find an average shift in potential of approximately − 120 mV, when compared to unmodified PEDOT:PSS. Here we have used a gold tip and calibrated the microscope with a gold film. We find the gold film has a surface potential of approximately 30 mV. We measure an average shift in potential for the PEDOT:PSS and G-PEDOT:PSS films of 850 and 730 mV, respectively. A gold sample freshly evaporated under ultra high vacuum has a work function of approximately 5.1 eV [21]. However, the exact environment and surface condition of the gold calibration sample and tip may significantly affect its work function, giving an uncertainty in the absolute values of the surface potentials we can estimate for the PEDOT:PSS samples. Here our gold sample was evaporated under ultra high vacuum, transferred to the Kelvin probe rig under nitrogen and stored under ultra high vacuum for a number of years. Hansen et al. have shown that the work function of gold can decrease to 4.7–4.8 eV depending upon its environment [22]. Using this lower value of the gold work function we estimate the work functions of PEDOT:PSS and G-PEDOT:PSS to be approximately 5.5 and 5.4 eV, respectively. These values are similar, though a little higher to those reported in literature for the PEDOT:PSS system [23]. The higher

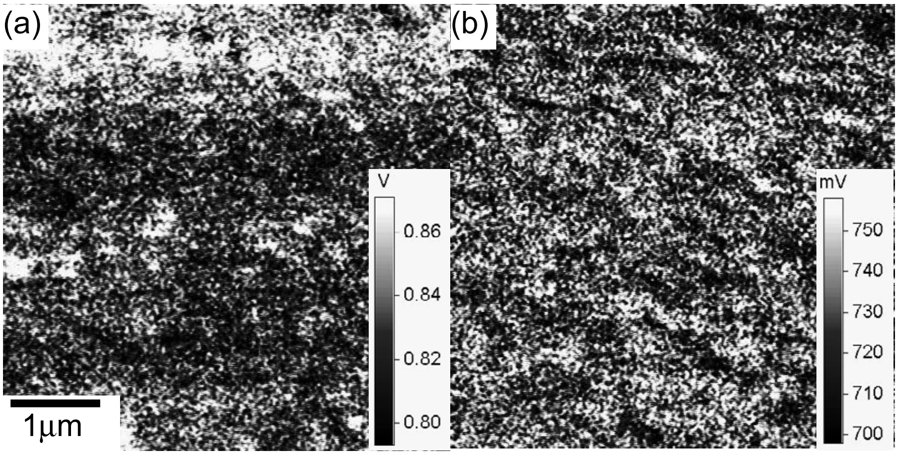

Fig. 4. Kelvin probe microscopy surface potential images of: (a) PEDOT:PSS and (b) G-PEDOT:PSS films spin-coated on ITO-coated glass slides.

values reported here are likely to be due to the excess PSS we have in this system. We also performed macroscopic Kelvin probe measurements and found a similar shift in surface potential of the G-PEDOT:PSS when compared to the PEDOT:PSS.

We fabricated symmetric ‘hole-transporting’ diodes with a structure from bottom to top of Au/PEDOT:PSS/PFB/PEDOT:PSS/Au and Au/G-PEDOT:PSS/PFB /G-PEDOT:PSS/Au. We find asymmetric diode behaviour for the current voltage characteristics of the PEDOT:PSS diode, having a rectification ratio of 3 at ±2 V. However, the G-PEDOT:PSS device exhibits negligible rectification, Fig. 5.

Photovoltaic diodes comprising PEDOT:PSS or G-PEDOT:PSS anodes, a blend of PFB:F8BT 1:1, as the photoactive layer, and aluminium cathodes were fabricated and tested. The photovoltaic action spectra for the diode with the G-PEDOT:PSS anode shows a significant improvement when compared to a similar device with a PEDOT:PSS anode, Fig. 6. Further to improvement in the external quantum efficiency, the open-circuit voltage of devices with G-PEDOT:PSS anodes is marginally higher than that of PEDOT:PSS anodes (1.3 V as opposed to 1.1 V).

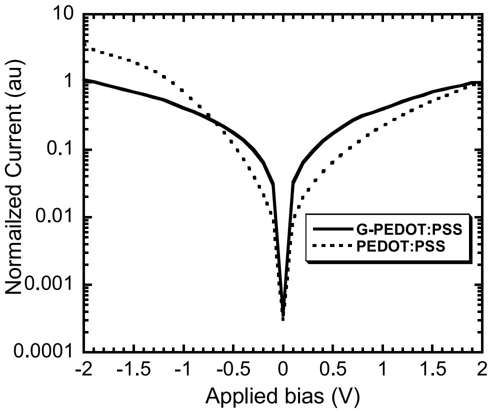

Fig. 5. Current–voltage curves for devices fabricated with Au/PEDOT:PSS/PFB/PEDOT:PSS/Au (dotted line) and Au/G-PEDOT:PSS/PFB /G-PEDOT:PSS/Au (solid line). The PFB films were 100 nm thick and the PEDOT:PSS and G-PEDOT:PSS films were 50 nm thick. The curves have been normalized at +2 V for ease of comparison. Negative bias corresponds to hole injection from the bottom PEDOT:PSS film, and positive bias corresponds to hole injection from the top PEDOT:PSS film.

4. Discussion

Phase segregation has been shown to occur in the PEDOT:PSS system. The dry colloidal particles consist of a core shell morphology with a PSS-rich shell [13]. Furthermore, the spin-coated PEDOT:PSS film vertically segregates, macroscopically, leading to a PSS-rich surface layer [14,15]. This can be expected when a binary mixture is made into a thin film. The interaction between the two components and the substrate or the atmosphere has to only vary slightly for the mixture to stratify [24].

The increased conductivity measured for the G-PEDOT:PSS film is consistent with previous findings. The AFM images of PEDOT:PSS and G-PEDOT:PSS films suggest that the polymer nanoparticles swell and aggregate together

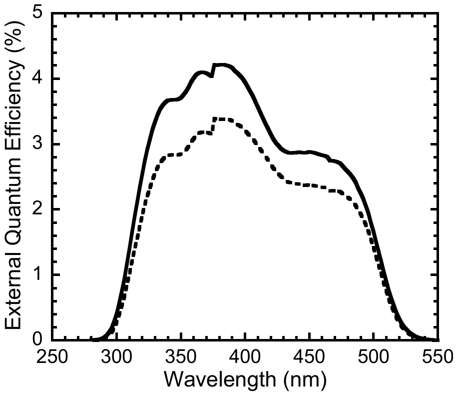

Fig. 6. Photovoltaic action spectra for PFB:F8BT 1:1 blend devices with PEDOT:PSS (dotted line) and G-PEDOT:PSS (solid line) anodes.

in the film forming process in the presence of glycerol, Fig. 2. It has been suggested that glycerol may act as a plasticiser, upon addition to PEDOT:PSS [25]. On the nano-length-scale there may be little or no change to the structure. However, mesoscopically there is likely to be improved connectivity between conductive regions. The 'swollen' colloidal particles, in effect increase the volume fraction of conductive regions. By considering the limiting factor to charge transport being hopping between these highly conductive regions, we may expect the modified film to have much improved charge percolation pathways.

Fourier transform infrared spectroscopy has ruled out glycerol still being present in the G-PEDOT:PSS films after the annealing process. This indicates that all electronic changes are due to structural reorientations. This is in agreement with Patterson et al. who found no sorbitol (a high boiling point alcohol also found to improve the conductivity of PEDOT:PSS) to be left in the PEDOT:PSS film after annealing [25].

Kelvin probe microscopy is an effective tool for mapping the surface potential of a material, and furthermore the technique is highly sensitive to the presence of surface dipoles. We see a significant shift in potential of −120 mV for the G-PEDOT:PSS film as compared to the PEDOT:PSS film, Fig. 4. The work function of PEDOT is less than that of the PEDOT:PSS blend, and the work function of PEDOT:PSS increases upon the addition of more PSS [26,27]. Thus, this shift in surface potential is consistent with a reduction in the surface enrichment of PSS. Suggesting that the G-PEDOT:PSS film has improved mixing macroscopically within the plane of the film, as well as on the length scale of the polymer nanoparticles. As stated earlier, the exact work function of a metal, in this case gold, will vary considerably depending upon its prior treatment and storage conditions. Thus, the surface potentials calculated are not necessarily an accurate reflection of the work functions, however, the relative potential shift between samples is reliable. It is also significant to note that PSS has a net negative charge and PEDOT has a net positive charge. Although PEDOT:PSS has metallic characteristics it is still intrinsically a semiconductor and thus it is possible for a net charge density to build up within the film. Thus the more negative surface potential of the PEDOT:PSS film is consistent with surface enrichment of PSS if a surface dipole is generated.

It has been shown that the hole injection from PEDOT:PSS into polymer films can be greatly improved by creating a gradient of PSS concentration, with a PSS-rich top (injecting) surface [27]. By looking at the current voltage characteristics of devices with PEDOT:PSS as both the cathode and the anode, we can infer the structure of the electrodes by considering the relative efficiency of hole injection. It is apparent that the device with PEDOT:PSS as the anode and cathode has improved injection from the bottom electrode (negative bias), Fig. 5. This is consistent, as we would expect the PEDOT:PSS film to have an enrichment of PSS at the surface. This should aid charge injection into the PFB by gradually increasing the work function from the ITO surface to the PFB surface giving a graduated barrier to hole injection [27]. Injection from the top electrode (positive bias) will not be aided by the PSS surface enrichment as hole injection occurs through the underside of the film, this will thus present a larger barrier to hole injection, as measured. The device with G-PEDOT:PSS anode and cathode, on the other hand, shows symmetric charge injection characteristics. This suggests uniform film composition within the plane of the film. These finding are in agreement with recently published work by Jönsson et al. who show via the use of use photo electron spectroscopy that a solvent treated (sorbitol, NMP and isopropanol) PEDOT:PSS film no longer has a PSS enrichment at the surface [28]. It is important to note, that although the conductivity of the PEDOT:PSS is greatly improved upon the addition of glycerol, the charge injection properties into the photoactive material may not be. This has severe implications for the use of high conductivity PEDOT:PSS as the hole-injection electrode for light emitting diodes.

The external quantum efficiency for a 1:1 PFB:F8BT blend photovoltaic device, comprising a G-PEDOT:PSS anode shows a significant improvement when compared to a similar device with a PEDOT:PSS anode, Fig. 6. We believe this to be due to improved charge collection from the G-PEDOT:PSS anode. The work function of PEDOT:PSS is known to be close to the highest occupied molecular orbital (HOMO) energy level of PFB. This leads to good hole-injection, due to the lack of an injection barrier, from the highly doped film into PFB. However, this suggests that there may be a barrier to charge collection. By reducing the surface potential, through improved blending from the addition of glycerol, we increase the injection barrier from the PEDOT:PSS into PFB and thus reduce the hole-injection barrier from PFB into the PEDOT:PSS anode, see Fig. 7 for illustration. This is likely to improve the charge collection efficiency as there will be less build up of space charge near the anode.

We have previously demonstrated that the open-circuit voltage of a polymer blend photovoltaic device can be increased by increasing the barrier to charge injection from

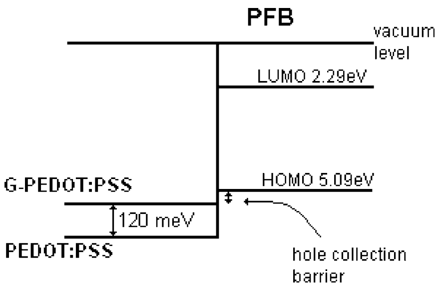

Fig. 7. The energy level diagram for PEDOT:PSS, G-PEDOT:PSS and PFB. The change in the PEDOT:PSS work function upon addition of glycerol is illustrated. The PFB energy levels are taken from literature [30].

the electrodes into the photoactive layer [29]. This is the physical consequence of increasing the shunt resistance of the theoretical photodiode circuit. The increase in open-circuit voltage measured when the anode is modified with glycerol once again illustrates the increase in the barrier to hole injection from the PEDOT:PSS into the PFB.

5. Conclusion

The addition of glycerol to a PEDOT:PSS solution prior to spin-coating reduces the sheet resistivity of the dried films by three orders of magnitude. There is no glycerol present in the film, after the heat treatment, and the improved conductivity is due to swelling and aggregation of the colloidal PEDOT-rich particles, forming a highly conductive network. However, this is not the only electronic consequence of such modification. From Kelvin probe microscopy, we find the surface potential of the PEDOT:PSS film decreases by approximately 0.12 eV upon the addition of glycerol. Photovoltaic devices fabricated with G-PEDOT:PSS anodes (in conjunction with ITO) show significant improvement when compared to devices with PEDOT:PSS anodes. This improvement can be assigned to the reduction of the anode work function, in turn reducing the hole injection barrier from the PFB into the PEDOT:PSS. Significantly, a method to improve the conductivity of the polymer anode has resulted in substantially altering other semiconductor properties.

Acknowledgements

This work was supported by the Engineering and Physical Sciences Research Council, (EPSRC) and the Kelvin probe microscope was funded by the EPSON Cambridge laboratory.

References

[1] Brabec CJ, Sariciftci NS, Hummelen JC. Adv Funct Mater 2001; 11(1):15–26.

[2] www.cdtltd.co.uk

[3] Halls JM, Arias AC, Mackenzie JD, Wu W, Inbasekaran M, Woo EP, Friend RH. Adv Mater 2000;12(7):498–502.

[4] Arias AC, MacKenzie JD, Stevenson R, Halls JM, Inbasekaran M, Woo EP, Richards D, Friend RH. Macromolecules 2001;34(17): 6005–13.

[5] Roman LS, Mammo W, Pettersson LAA, Andersson MR, Inganäs O. Adv Mater 1998;10(10):774–7.

[6] Granström M, Petritsch K, Arias AC, Lux A, Andersson MR, Friend RH. Nature 1998;395:257–60.

[7] Groenendaal LB, Jonas F, Freitag D, Pielartzik H, Reynolds JR. Adv Mater 2000;12(7):481–94.

[8] Scott JC, Carter SA, Karg S, Angelopoulos M. Synth Met 1997;85(1-3):1197–200.

[9] Kim JS, Lagel B, Moons E, Johansson N, Baikie ID, Salaneck WR, Friend RH, Cacialli F. Synth Met 2000;111:311–4.

[10] Nyberg T. Synth Met 2004;140(2-3):281–6.

[11] Kim WH, Mäkinen AJ, Nikolov N, Shashidhar R, Kim H, Kafafi ZH. Appl Phys Lett 2002;80(20):3844–6.

[12] Zhang F, Johansson M, Andersson MR, Hummelen JC, Inganäs O. Adv Mater 2002;14(9):662–5.

[13] Greczynski G, Kugler Th, Keil M, Osikowicz W, Fahlman M, Salaneck WR. J Electron Spectrosc 2001;121(1-3):1–17.

[14] Jones RAL. Cambridge Optoelectronics Group Seminar; 2003.

[15] Greczynski G, Kugler Th, Salaneck WR. Thin Solid Films 1999;354: 129–35.

[16] Snaith HJ, Arias AC, Morteani AC, Silva C, Friend RH. Nanoletters 2002;2(12):1353–7.

[17] Bürgi L, Sirringhaus H, Friend RH. Appl Phys Lett 2002;80(16): 2913–5.

[18] Corcoran N, Arias AC, Kim JS, MacKenzie JD, Friend RH. Appl Phys Lett 2003;82(2):299–301.

[19] Aleshin AN, Williams SR, Heeger AJ. Synth Met 1998;94(2):173–7.

[20] Colthup NB, Daly LH, Wilberley SE. Introduction to infrared and Raman spectroscopy. 3rd ed. London: Academic Press; 1990. Chapter 10.

[21] Weast RC. Handbook of chemistry and physics. 66th ed. New York: Chemical Rubber; 1995. E-86.

[22] Hansen WN, Johnson KB. Surf Sci 1994;316(3):373–82.

[23] Brown TM, Kim JS, Friend RH, Cacialli F, Daik R, Feast WJ. Appl Phys Lett 1999;75(12):1679–81.

[24] Kim JS, Ho PKH, Murphy CE, Friend RH. Macromolecules 2004;37: 2861–71.

[25] Pettersson LAA, Ghosh S, Inganäs O. Org Elec 2002;3(3–4):143–8.

[26] Xing KZ, Fahlman M, Chen XW, Inganäs O, Salaneck WR. Synth Met 1997;89(3):161–5.

[27] Ho PKH, Kim JS, Burroughes JH, Becker H, Li SFY, Brown TM, Cacialli F, Friend RH. Nature 2000;404:481–4.

[28] Jönsson SKM, Salaneck WR, Fahlman MJ. Electron Spectrosc 2004; 137–140:805–9.

[29] Snaith HJ, Greenham NC, Friend RH. Adv Mater 2004;16(18): 1640–5.

[30] Redecker M, Bradley DDC, Inbasekaran M, Wu WW, Woo EP. Adv Mater 1999;11(3):241–6.